Received: 22 December 2022 | Revised: 5 April 2023 | Accepted: 20 April 2023

DOI: 10.1002/hyp.14893

RESEARCH ARTICLE

WILEY

Model-coupled GRACE-based analysis of hydrological dynamics of drying Lake Urmia and its basin

Behnam Khorrami[1] | Shoaib Ali[2] | Onur Gungor Sahin[3] | Orhan Gunduz[4]

[1]Department of GIS, The Graduate School of Natural and Applied Sciences, Dokuz Eylul University, Izmir, Turkey

[2]School of Water Conservancy and Civil Engineering, Northeast Agricultural University, Harbin, China

[3]Department of International Water Resources, Izmir Institute of Technology, Izmir, Turkey

[4]Department of Environmental Engineering, Izmir Institute of Technology, Izmir, Turkey

Correspondence
Behnam Khorrami, Department of GIS, The Graduate School of Natural and Applied Sciences, Dokuz Eylul University, Izmir, Turkey.
Email: behnam.khorrami@ogr.deu.edu.trc

Abstract

Lake Urmia basin (LUB), in northwestern Iran, is under the influence of extreme degradation due to a number of natural and anthropogenic factors. The existence of the Lake is critical for the microclimate of the region as well as the quality of human life and wildlife, which necessitates an up-to-date and holistic analysis of its hydrological dynamics. In this premise, satellite-based terrestrial water storage (TWS) received from the Gravity Recovery and Climate Experiment (GRACE) mission was coupled with hydrometeorological modelling and assessment tools to analyse the hydrological status of the lake and its basin. As a new gap-filling approach, the Seasonal-Trend decomposition using Locally estimated scatterplot smoothing (LOESS) (STL) decomposition technique was proposed in this study to reconstruct the missing TWS data. Integrating satellite precipitation data with the Catchment Land Surface Model (CLSM) and WaterGAP model outputs, the hydrological status of the lake was investigated. The STL-based TWS turned out to concord well with the simulated TWS from the CLSM indicating the acceptable performance of the proposed technique. The findings revealed that the LUB had undergone an alarming hydrological situation from 2003 to 2021 with a total loss of 10 and 7.56 km^3 from its TWS and groundwater storage (GWS), respectively. The water level time series also indicated that the water level of the lake had diminished with an annual rate of -70 ± 21 cm/year corresponding to a total water level depletion of about 13.35 ± 3.9 m during the 2003–2021 period. The GRACE-derived TWS and GWS also agreed well with the CLSM simulations. Assessment of the extreme events of the LUB suggested that the basin suffered from a severe dry event in 2008 resulting in the depletion of its water storage and water level. It was also found that from 2003 onward, a critical hydrological setting had dominated the LUB with a negative hydrological balance of -0.96 km^3.

KEYWORDS

desiccation, gap filling, GRACE, Lake Urmia basin, seasonal-trend decomposition using LOESS, terrestrial water storage

1 | INTRODUCTION

As one of the largest Middle-Eastern countries, Iran's climate is of arid to semi-arid type. This generic aridity accompanied by the large-scale impacts of climate change, population growth, urban development and the national policy of food self-sufficiency has culminated in the detriment of its surface and subsurface water bodies by the increased pressure on the water resources of the country (Forootan et al., 2014). The climate crisis resulted in severe impacts in most of its regions and manifested itself in terms of increasing temperatures, diminishing precipitation and consequently, decreasing availability of renewable water resources (Hosseini-Moghari et al., 2020). The increasing population has ramifications for water resources escalating the need for fresh water in populated centres and agricultural lands (Forootan et al., 2014). Several water bodies in Iran including wetlands and lakes have dried out and groundwater aquifers have degraded dramatically in different parts of the country (Hosseini-Moghari et al., 2020; Khorrami & Gunduz, 2019; Madani et al., 2016). Less than 10% of Iran's territory benefits from sufficient precipitation, while the majority of the country (more than 90%) is affected by the associated side effects of an arid to semi-arid climate, and therefore, is mainly dependent on groundwater aquifers to meet the required water demands (Forootan et al., 2014). The overexploitation of groundwater in recent decades has resulted in the rapid degradation of several aquifers and groundwater-related surface water bodies throughout the country. Due to low social awareness regarding the status and importance of groundwater and groundwater-dependent eosystems, the diminishing groundwater level is deemed an invisible disaster in the country (Hosseini-Moghari et al., 2020).

The Lake Urmia basin (LUB) in northwestern Iran is among the most important basins in the country regarding its hydrological status. The water level and the associated storage in Lake Urmia (LU) have been subjected to a severe decline in recent years, which is strongly related to both anthropogenic and natural forces. To date, several researchers have investigated the variations of water storage over the LUB based on numerous approaches and reported the influential factors responsible from the drying of the Lake including decreased precipitation, increased temperature and evapotranspiration, development of new agricultural land, excessive extraction of groundwater, construction of man-made water diversion structures and building a causeway across the lake (Banihabib et al., 2015; Farajzadeh et al., 2014; Fathian et al., 2015; Jalili et al., 2012; Kamran & Khorrami, 2018; Zeinoddini et al., 2009). Known as one of the biggest saline lakes in the world, the LU has lost most of its water storage in recent years. Figure SM1 demonstrates the spatiotemporal evolution of the desiccation process in the LU from 2003 to 2020. In light of the unique role that the LU plays in sustaining the microclimate of the region (Azizpour & Ghaffari, 2021), exact and regular monitoring of its water storage and detection of the influential parameters in the variations of the lake water storage bear the utmost importance.

Remote sensing observations provide unique means for the distant estimation and evaluation of different environmental phenomena, especially over large scales, for which in-situ data are either inaccessible or insufficient. One of the recent high-tech achievements in the field of environmental remote sensing satellites is the Gravity Recovery and Climate Experiment (GRACE) mission, through which large-scale variations of the main hydrological compartments can be estimated. The GRACE mission is the only remote sensing system capable of measuring water storage changes at all levels beneath and on the land surface, through which an unprecedented opportunity is offered to understand and improve the simulation of terrestrial water storage (TWS) variability (Zaitchik et al., 2008). However, the GRACE-observed data are associated with missing values, which impede a comprehensive and uninterrupted analysis of hydrological components. Therefore, a reconstruction of GRACE data is vital within the scope of any GRACE-based analysis. Although the GRACE gap filling is a relatively new topic, several techniques including data-driven methods (Li et al., 2020), automatic machine learning (Sun et al., 2021), deep learning (Sorkhabi et al., 2021; Uz et al., 2022), multichannel singular spectrum analysis (Wang et al., 2021), Neural Networks (Lai et al., 2022; Mo et al., 2022; Zhang, Yao, & He, 2022), and physically based reconstruction (Zhang, Li, et al., 2022) have so far been implemented to fill in the gaps of the GRACE/GRACE-Follow-On (GRACE-FO) estimates. However, the complexity of the used techniques and the necessity to use auxiliary data to simulate the missing TWS is still a major challenge associated with these techniques.

Based on this premise, a new technique is proposed in this study to bridge the gaps within and between the GRACE and GRACE-FO observations in a more convenient way. To this end, the Seasonal-Trend decomposition using Locally estimated scatterplot smoothing (STL) was applied to reconstruct the missing TWS values from 2003 to 2021 over the LUB. The gap-free GRACE/GRACE-FO data were then used alongside other remote sensing and modelled data to systematically investigate the hydrological dynamics of the drying LU to uncover the variations of its water storage and water level and to evaluate the anthropogenic and natural parameters responsible from the lake's desiccation in recent decades.

2 | SITE DESCRIPTION

Lake Urmia (LU) is the largest inland lake in Iran and the Middle East, and the second-largest hypersaline lake in the world (Vaheddoost & Aksoy, 2019). It is a Ramsar Site and a UNESCO Biosphere Reserve and is designated as a national park due to its ecological and natural features (Hosseini-Moghari et al., 2020). The lake is at an altitude of 1250 m above sea level with a maximum water depth of 16 m. The LU is divided into two (i.e., northern and southern) parts separated by a causeway and a 1500 m bridge that allows only limited water exchange between these two sections. The LU stretches about 140 km in length, from north to south, and 50 km in width, from east to west, (Azizpour & Ghaffari, 2021). The LUB covers about 51 800 km^2 in the northwest region of Iran (Figure 1a) hosting an estimated population of 7 million (10% of Iran's population) (Feizizadeh et al., 2021). Different land use/cover (LULC) classes such as bare

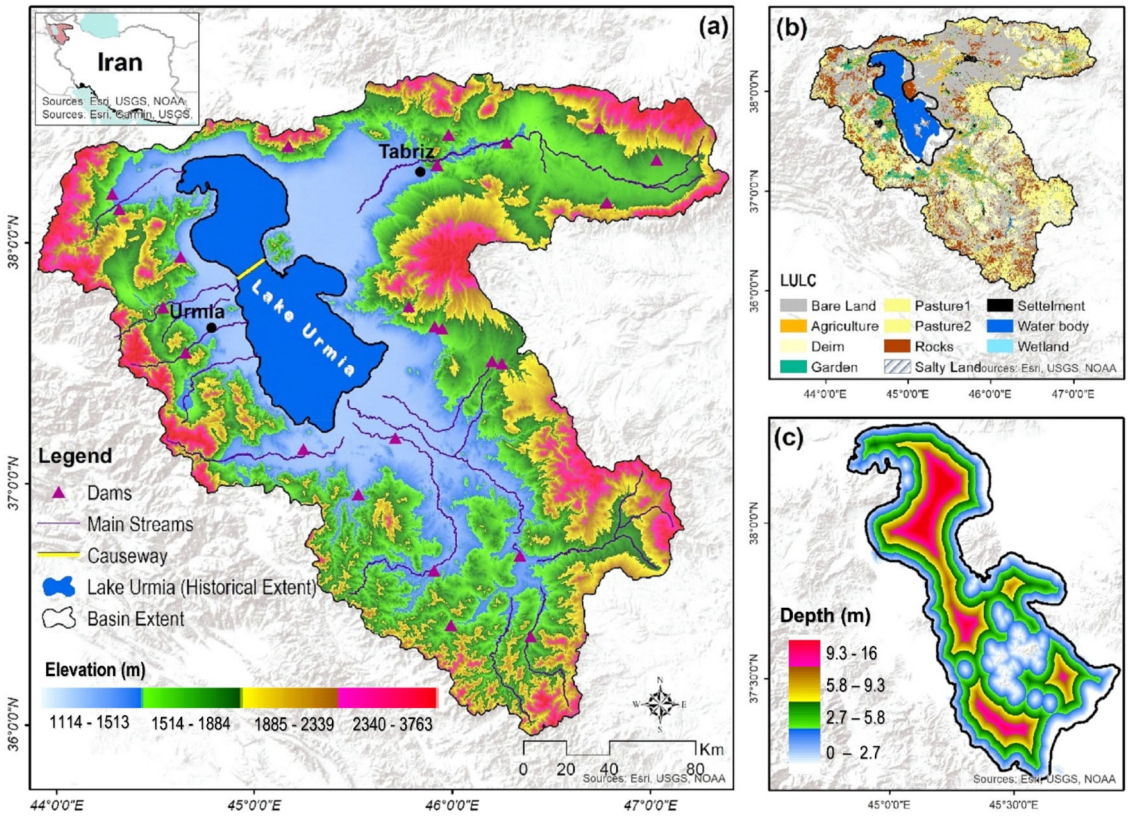

FIGURE 1 The geographic location of Lake Urmia and its basin in NW Iran (a), land use/cover (LULC) (b), and the lake's bathymetry (c).

land, pasture, agricultural lands, wetlands, orchards, rocks and sediments are distinguished in the basin (Figure 1b). The LUB is composed of 68 streams/rivers of which 56 are intermittent streams/rivers contributing to the water inflow into the LUB (Hosseini-Moghari et al., 2020). The construction of dams on these streams supplying water to LU, over-exploitation of groundwater for various anthropogenic purposes as well as the increased frequency of hydrometeorological extremes have resulted in the reduced annual water input to the lake. The bathymetry map of the LU (Figure 1c) indicates that the depth of the lake ranges from a minimum of 0 m to a maximum of 16 m, which is a clear indication of the shallow character of the lake.

3 | METHODOLOGY

3.1 | Datasets

3.1.1 | GRACE and GRACE-FO observations

The GRACE is a pioneering remote sensing project, which consists of two co-orbiting satellites to gather the gravitational signals of the Earth (Khorrami & Gunduz, 2021a). The project was started by launching the first set of satellites in March 2002. The GRACE-1 (called GRACE) satellite continued recording the gravity field for 16 years and terminated its mission in June 2017. After an 11-month delay, the second mission was started by placing the GRACE-FO in the Earth's orbit in May 2018 (Khorrami et al., 2021). These two missions have been providing the public end-users with invaluable data on the monthly anomalies of Terrestrial Water Storage (TWS) processed by different centres. The primary data format of the GRACE mission is Spherical Harmonics (SH) signals that require postprocessing. The latest data format of the mission is called Mass Concentration (Mascon) blocks, which are post-processed and ready to use. Moreover, the Mascon solutions are global and not tailored towards a particular application, and hence, they can be utilized for all scientific topics of interest (Save et al., 2016). Hence, in this study, the latest release of the GRACE/GRACE-FO Mascon solutions including CSR, JPL and GSFC Mascons was utilized. The TWS data can be downloaded from http://www2.csr.utexas.edu/grace/RL06_Mascons.html (for CSR data), and https://earth.gsfc.nasa.gov/geo/data/grace-Mascons (for JPL and GSFC data).

3.1.2 | Global Land Data Assimilation System model

The Global Land Data Assimilation System (GLDAS) is a widely utilized large-scale hydrological model established by NASA and the National Centres for Environmental Prediction. Within the framework of this model, different hydrometeorological variables are simulated by integrating some in-situ and satellite observations at a higher resolution. The GLDAS utilizes advanced land surface models (LSMs), such as Community Land Model (CLM), Variable Infiltration Capacity (VIC)

model, Noah model, Mosaic model and Catchment land surface model (CLSM), to simulate the land surface states and fluxes (Hu et al., 2019). The CLSM is the only model of the GLDAS and also one of the few global models to simulate ground water storage (GWS) (Girotto et al., 2021). In this study, the simulated variables of Soil Moisture Storage (SMS), Snow Water Equivalent (SWE), Surface Water Storage (SMS) and Evapotranspiration (ET) were received from the Noah model. The TWS and GWS were extracted from the CLSM model and were integrated into the analysis. The GLDAS data is accessible from https://ldas.gsfc.nasa.gov/gldas.

3.1.3 | WaterGAP model

The WaterGAP is one of the pioneering hydrological modelling missions developed with the primary motivation of quantifying large-scale (regional to global) water resources by concentrating on the anthropogenic impacts to evaluate water stress (Khorrami, Ali, et al., 2022). The model utilizes water use models to simulate the volume of water consumption in different sectors (Portmann, 2017). The grid-wise water simulations of the WaterGAP agree well with the global data (Alcamo et al., 2003). In this study, the total water consumption from the surface and subsurface water resources was extracted from 0.5-degree resolution WaterGAP model outputs. The WaterGAP model data is accessible at https://www.uni-frankfurt.de/45218093/Global_Water_Modeling.

3.1.4 | Climate Hazards Group Infrared Precipitation with Station data

Climate Hazards Group Infrared Precipitation with Station data (CHIRPS) dataset is a relatively new quasi-global, high-resolution, daily/monthly precipitation dataset. Being known as one of the most accurate gridded precipitation datasets, CHIRPS is often used as an alternative source of precipitation measurements, especially where sufficient measurements are not accessible (Paca et al., 2020). The CHIRPS monthly precipitation data with a resolution of 0.05° can be downloaded from http://chg.geog.ucsb.edu/data/chirps/.

3.1.5 | In-situ observations

The long-term observations of the water level of the LU were received from the portal of the Lake Urmia Research Plan (LURP) and can be downloaded from https://b2n.ir/y26109.

3.2 | Drought metrics

In this study, global drought indices including the Standardized Precipitation-Evapotranspiration Index (SPEI) and Self-calibrating Palmer Drought Severity Index (scPDSI) were utilized to evaluate hydrometeorological extremes over the LUB. The scPDSI and SPEI are water balance-based drought indices. scPDSI is a revised form of PDSI, through which historical precipitation and temperature data are integrated into the soil characteristics to assess extreme incidents (Briffa et al., 2009). SPEI, on the other hand, is a multiscale indicator calculated based on the deviation of precipitation and evapotranspiration records (Beguería et al., 2010). The integration of evapotranspiration into the calculation process is the unique aspect of the SPEI, through which the evaporative demand is applied to better describe the global hydrometeorological extremes (Beguería et al., 2010). The monthly scPDSI and SPEI were downloaded from (https://www.uea.ac.uk/web/groups-and-centres/climatic-research-unit/data) and (https://digital.csic.es/handle/10261/268088), respectively. The characteristics of the data used in this study are given in detail in Table 1.

3.3 | Methods

In this study, the STL technique was utilized to reconstruct the missing TWS values of the GRACE/GRACE-FO missions. The seamless TWS data were then integrated with model outputs to estimate GWS. The GRACE-based TWS and GWS were then compared with model-based TWS and GWS. The lake's water level data were then associated with the variations of the GRACE-derived TWS. The hydrologic dynamics of the lake were then investigated in term of anthropogenic and natural processes by the integrated analysis of the satellite- and model-based observations. The overall schematic flow of the research analysis is given in Figure 2.

3.3.1 | STL-based GRACE gap filling

The TWS data received from the GRACE and the GRACE-FO missions suffer from periodic intra-gaps (within the GRACE mission) and continuous inter-gaps (between the two missions) (Flechtner et al., 2014; Yi & Sneeuw, 2021). These missing values hinder better monitoring of water resources. Therefore, it is a must to fill in the missing data for an accurate assessment of hydrological cycle components. Overall, there are 36 missing months in GRACE data from 2002 to 2021 (Figure SM2). The TWS observations manifest seasonal variations with a long-term trend. This common facet of the GRACE-observed TWS was addressed and the gaps of the GRACE/GRACE-FO observations were filled in based on Seasonal-Trend decomposition using Locally estimated scatterplot smoothing (LOESS) (STL) to have a complete set of the GRACE/GRACE-FO data. In this premise, a simple additive decomposition model is executed in the R programming environment to fill in the missing data. The STL model decomposes the data into trend, seasonal and residual components.

$$TWS_t = T_t + S_t + R_t, \quad (1)$$

where TWS_t is the terrestrial water storage at time t; T, S and R denote the trend component, the seasonal component, and the

TABLE 1 Specifications of the datasets used in the study.

Mission	Data type	Resolution Temporal	Spatial
GRACE/GRACE-FO	Satellite	Monthly (2003–2021)	CSR: 0.25° × 0.25° JPL: 0.5° × 0.5° GSFC: 0.5° × 0.5°
GLDAS	Model	Noah: Monthly CLSM: Daily (2003–2021)	0.25° × 0.25°
WaterGAP	Model	Monthly (2003–2015)	0.5° × 0.5°
CHIRPS	Satellite	Monthly (2003–2021)	0.05° × 0.05°
Drought metrics	Model	Monthly (2003–2021)	0.05° × 0.05°
Lake water level	In situ	Monthly (2003–2021)	–

FIGURE 2 Schematic flow of the analysis.

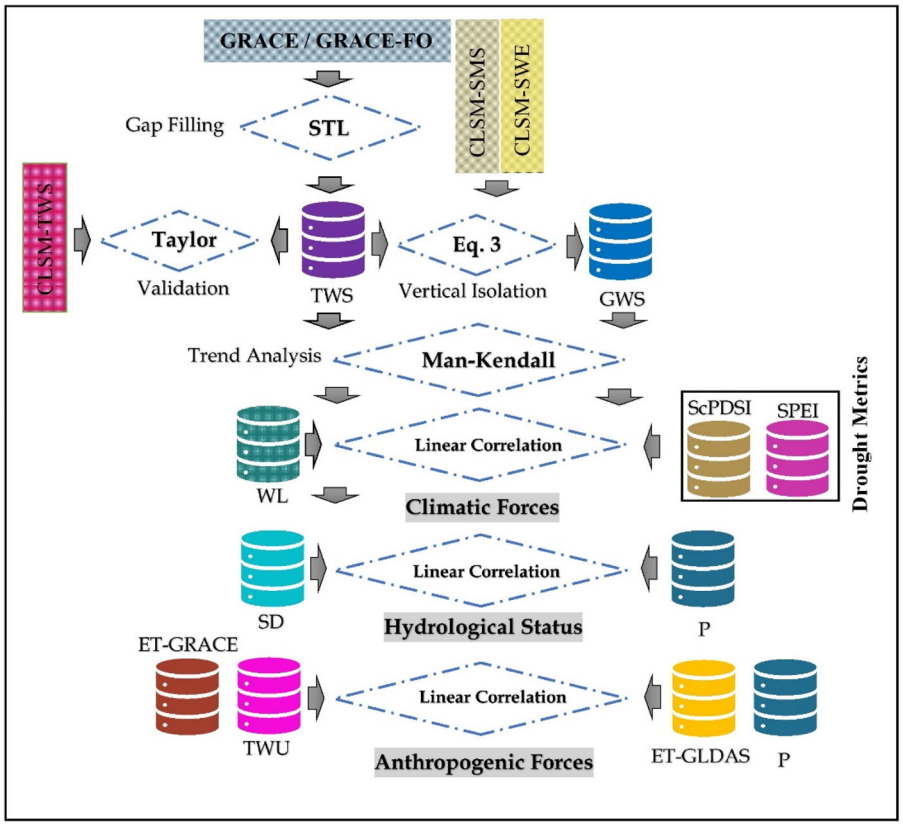

remainder component, respectively (Cleveland et al., 1990). The missing data were filled in using the trend from the decomposition of TWS, then added the average monthly and residual values of that month to calculate the missing months.

3.3.2 | Disintegration of TWS

TWS is a vertically integrated hydrological variable that encompasses the water storage anomalies of the soil moisture (SMS), snow water (SWE), groundwater (GWS) and surface water (SWS) (Khorrami & Gunduz, 2021b). The variations of groundwater storage can be extracted through the GRACE isolation process. Equations (2) and (3) describe the structure of TWS and the extraction of GWS, respectively.

$$\mathrm{TWS} = \mathrm{GWS} + \mathrm{SWE} + \mathrm{SMS} + \mathrm{SWS}, \tag{2}$$

$$\mathrm{GWS} = \mathrm{TWS} - [\mathrm{SWE} + \mathrm{SMS} + \mathrm{SWS}]. \tag{3}$$

3.3.3 | Mann-Kendall trend test

The Mann-Kendall (MK) technique (Kendall, 1975; Mann, 1945) was utilized to unearth the trend of the time series. The MK is a non-parametric statistical test, for which no distribution of the input

variables is required (Alhaji et al., 2018). Therefore, it is commonly utilized for trend analysis of the time series of hydro-meteorological variables (Tabari et al., 2011). The basic formulas of the MK technique are given in the Supplementary Material.

3.4 | Results

3.4.1 | STL gap-filling performance

The missing TWS values were filled in based on the STL technique in this study, which are then verified by the values obtained in the CLSM dataset. Today, the CLSM is the only global model, which makes use of the GRACE estimates in its sophisticated data assimilation process to generate hydrological fluxes (Kumar et al., 2016). As a result, spatiotemporally downscaled and gap-less values of TWS were simulated, which has culminated in improved estimates of hydrological components (Kumar et al., 2016). Therefore, the TWS results obtained from the STL method were validated against the CLSM-derived TWS over the LUB. Figure SM3 illustrates the performance accuracy of the proposed method in terms of the correlation between the missing values filled in with the STL technique and those derived from the CLSM. The results reveal that the used STL technique is successful in reconstructing the missing TWS values of the GRACE mission. According to the Taylor diagram, the correlation between the STL-based TWS and CLSM-TWS is 0.88, 0.89 and 0.91 for the JPL, GSFC and CSR data, respectively. The good performance of the proposed STL-based gap-filling approach is also verified by comparing it to the findings of previous studies. Soltani and Azari (2022) applied the Group method of data Handling (GMDH) machine learning technique to model TWS values over the LUB. According to Soltani and Azari (2022), the GMDH was considered a successful GRACE gap-filling technique that yields very good results in simulating the missing TWS values over the LUB with the best correlation of 0.73.

3.5 | Variations of TWS

Temporal variations of TWS over the LUB were drawn based on the basin-average TWS on the monthly scale (Figure 3). The variations of TWS over the LUB reveal that there is a high level of agreement between different GRACE solutions and the CLSM-TWS. The monthly variations (Figure 3a) of TWS manifest a strong association between CLSM and CSR, JPL and GSFC with a correlation of 0.91, 0.94 and

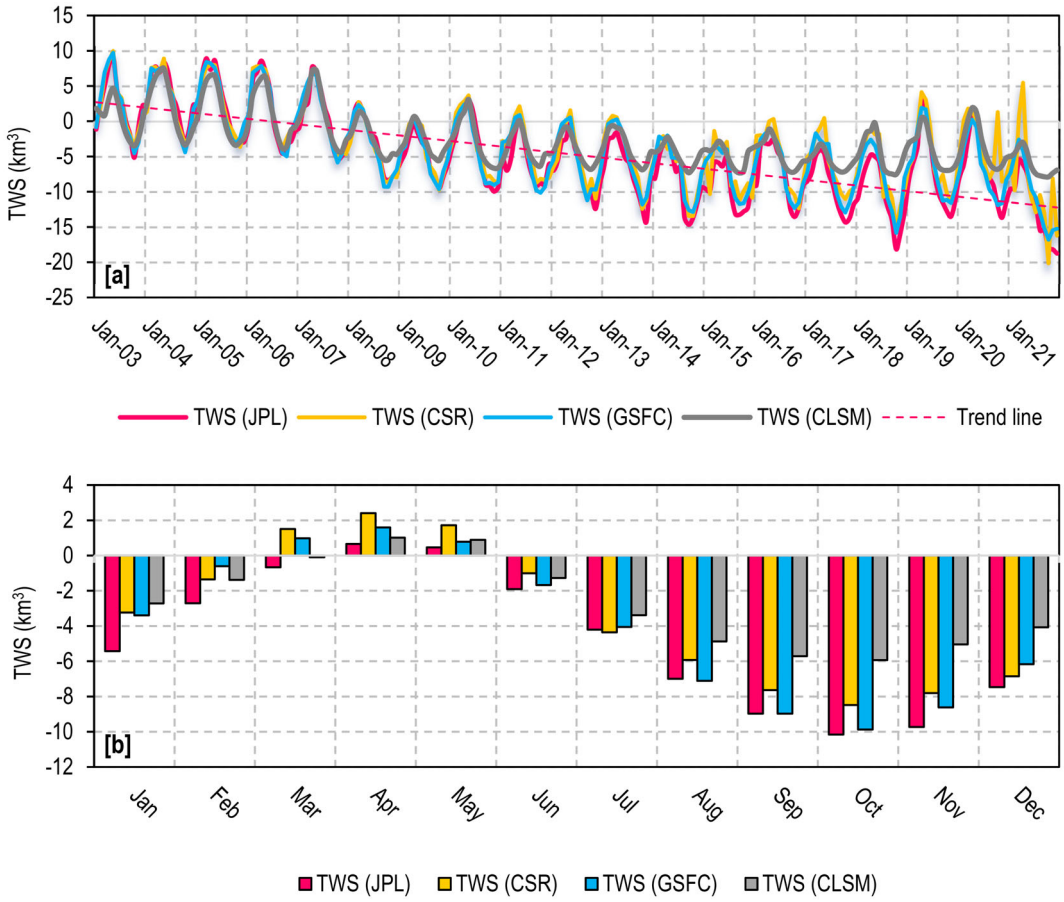

FIGURE 3 The multiyear (2003–2021) monthly (a) and mean-monthly (b) variations of terrestrial water storage (TWS) over Lake Urmia basin (LUB).

0.94, respectively. The climatology (mean monthly) variations (Figure 3b), on the other hand, show higher agreement between the GRACE and CLSM with a correlation of 0.99 (for the CSR), and 0.98 (for the JPL and GSFC). The monthly time series reveals that the CSR-TWS fluctuates between 9.96 km^3 (in May 2003) and −20.15 km^3 (in October 2021). The JPL-TWS fluctuates between 9.23 km^3 (in May 2003) and −18.76 km^3 (in October 2021), and the GSFC-TWS fluctuates between 9.72 km^3 (in May 2003) to −16.80 km^3 (in October 2021). The CLSM, on the other hand, shows TWS variations ranging from 7.50 km^3 (in May 2004) to −7.90 km^3 (in October 2021).

The mean monthly time series indicate that excluding March, April and May, during which positive TWS occurs over the basin, the variations of TWS are negative during the remaining months. The results indicate that in April the LUB experiences a maximum water storage surplus of 2.40 km^3 (CSR), 0.66 km^3 (JPL), 1.60 km^3 (GSFC) and 1.02 km^3 (CLSM). While the maximum storage loss turns out to occur during autumntime with the maximum depletion of −8.40 km^3 (CSR), −10.16 km^3 (JPL), −9.90 km^3 (GSFC) and −6.0 km^3 (CLSM) in October. The autumntime trough observed in the variations of TWS can be ascribed to the impacts of excessive water use for agriculture during the cultivation season (summertime). The variation pattern of TWS is in complete agreement with the findings of Humphrey et al. (2016), who reported the springtime and autumntime variations of the peak and trough values of TWS for the northern hemisphere of the world.

The spatial associations of the TWS derived from the GRACE solutions and the CLSM simulations are given in Figure SM4, according to which, the central and southern parts of the basin show a higher correlation with the CLSM while the northern parts manifest lower correlations. The correlation ranges from 0.79 to 0.94, and the RMSE ranges from 36 to 198 mm. It also suggests that the spatial distribution of the correlation and RMSE values are almost identical for the JPL- and CSR-derived TWS while the GSFC-TWS showcases a somehow different spatial pattern of correlation and RMSE compared to the JPL and CSR solutions.

3.6 | Variations of GWS

The variations of groundwater storage of the basin were extracted based on Equation 3 by integrating the hydrological components from the GLDAS-Noah model into the GRACE-TWS. The basin-wise variations of GWS based on the GRACE solutions and the CLSM model are given in Figure 4. According to the monthly variations of GWS (Figure 4a), the CSR, JPL and GSFC-derived GWS are in good agreement with the CLSM-derived GWS over the LUB. The temporal

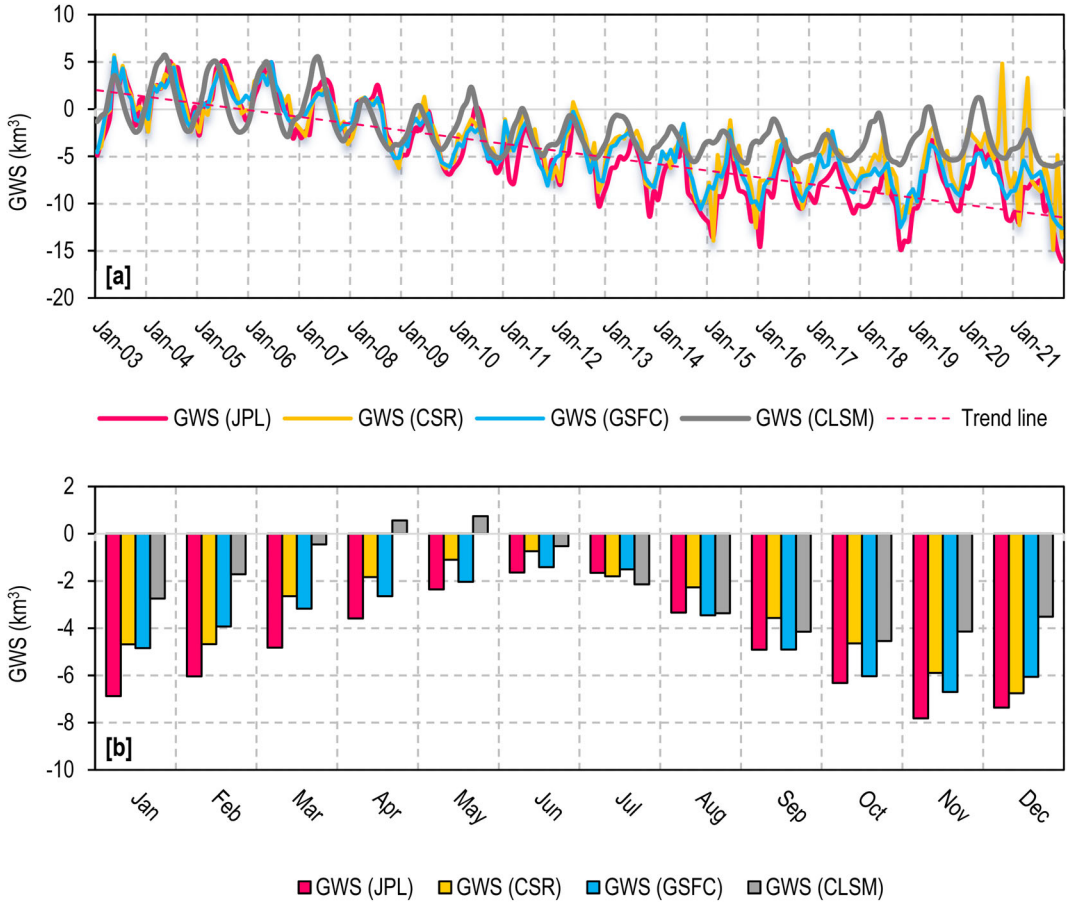

FIGURE 4 The multiyear (2003–2021) monthly (a) and mean-monthly (b) variations of groundwater storage (GWS) over the Lake Urmia basin (LUB).

correlation is 0.73, 0.76 and 0.79 for the CSR, JPL and GSFC, respectively. The mean monthly variations (Figure 4b), on the other hand, reveal that for the GWS variations, the association between the GRACE-GWS and CLSM-GWS is lower than that for the monthly variations. The temporal correlation of the climatology values is 0.70, 0.61 and 0.79 for the CSR, JPL and GSFC, respectively. Although the model-integrated disintegration of TWS may yield extra uncertainties of the extracted GWS (Sahour et al., 2020), a very high agreement between the GRACE-derived GWS and in-situ groundwater level of the LUB was reported from 2003 to 2019 (Saemian et al., 2020). This relatively low agreement between the GRACE-derived and CLSM-simulated GWS can be ascribed to the climatic setting of the study area. Shamsudduha and Taylor (2020) reported that the GWS uncertainty is generally higher for aquifer systems located in arid regions. Furthermore, the model-based simulation of GWS suffers from errors propagated from the uncertainty in the model computation and the data (Tangdamrongsub et al., 2018).

The monthly time series of GWS imply that the CSR-GWS fluctuates between 5.71 km^3 (in May 2003) and −14.90 km^3 (in October 2021). The JPL-GWS fluctuates between 5.10 km^3 (in June 2005) and −16.12 km^3 (in October 2021), the GSFC-GWS fluctuates between 5.46 km^3 (in May 2003) and −12.62 km^3 (in October 2021), and the CLSM-GWS fluctuates between 5.70 km^3 (in May 2004) and −6.50 km^3 (in October 2021). The mean monthly time series of GWS also indicate that except for April and May, during which there is a trivial increase in the groundwater storage of the basin detected only by the CLSM, the GRACE-derived GWS fluctuates negatively throughout the year from January to December. The variations of GWS (based on JPL) range from −1.64 km^3 (in June) to −7.82 km^3 (in November). The results indicate that in June the LUB experiences maximum groundwater storage of −0.74 km^3 (CSR), −1.64 km^3 (JPL), −1.41 km^3 (GSFC), and −0.55 km^3 (CLSM). While the maximum storage loss turns out to occur during autumntime with the maximum depletion of −5.90 km^3 (CSR), −7.82 km^3 (JPL), −6.70 km^3 (GSFC), and −4.15 km^3 (CLSM) in November. Similar to the TWS variations, the autumntime maximum GWS depletion of the basin can be associated with the impacts of excessive water use for agriculture during the cultivation season (summertime).

The spatial distribution of the correlation and RMSE values of the variations of GWS based on the GRACE solution and the CLSM model is illustrated in Figure SM5. The variations in the correlation and RMSE on a spatial domain suggest the same pattern for all the GRACE solutions over the LUB. The correlation between the GRACE-GWS and CLSM-GWS is the least in the western parts of the basin, which increases towards the east where it reaches 0.86. The distribution pattern for the RMSE of the GWS manifests an identical pattern for the CSR and GSFC and a different pattern for the JPL. The RMSE ranges from 36 to 192 mm.

3.7 | Trend analysis results

The MK-based estimated trend results are given in Table 2. The results demonstrate a decreasing trend for the TWS and GWS over the LUB. Overall, the estimated annual trends of TWS and GWS using the GRACE solutions and the CLSM simulations over the LUB are close to each other. The TWS variations based on the GRACE JPL, CSR and GSFC suggest a diminishing trend at a rate of −0.59, −0.46, and −0.53 km^3/year, respectively, which account for −11.20, −8.74 and −10.07 km^3 of total storage loss from 2003 to 2021. In the meantime, the CLSM-derived TWS manifests decreasing trend of −0.51 km^3/year, which is equal to −9.69 km^3 of total loss during the same period. The results also indicate that the LUB has suffered from an annual GWS loss of −0.47, −0.33, −0.40 and −0.53 km^3/year for the JPL, CSR, GSFC and CLSM, respectively, which account for the total groundwater depletion of −8.87, −6.22, −7.60 and −10.10 km^3, respectively. Overall and taking the mean values of the GRACE solutions into account, it can be stated that the LUB has lost about 10 and 7.56 km^3 of its TWS and GWS during the last 19 years from 2003 to 2021. Tourian et al., 2015 and Hosseini-Moghari et al. (2020) reported an estimated TWS loss of −8.0 km^3 (based on GRACE) and −9.9 km^3 (based on the WaterGAP model) from 2002 to 2014 and 2003 to 2013, respectively. In another study, the total GWS loss of the basin from 2002 to 2020 was estimated to be about −7.34 km^3 (Soltani & Azari, 2022), which is comparable to our findings.

3.8 | Water level variations and their associations with TWS

The variations in the lake's water level (Figure 5) were derived using the in-situ data. Like the TWS, the water level variations also reveal a descending trend from 2003 to 2021 with a rate of −70 ± 21 cm/year. The annual depletion rate of the lake's water level from 2002 to 2014 was −34 ± 1 cm/year (Tourian et al., 2015). The LU water level manifests a slightly increasing trend in 2016, and from 2019 to 2020, which is due to the increased precipitation and the water inflow from the reservoirs under the restoration program (Saemian et al., 2020). The time series on a monthly and mean monthly scale demonstrate a strong association between the variations of TWS and those of water level. The best correlation of 0.81 was observed for the JPL-TWS and water level. The correlation between the water level and CSR-, GSFC- and CLSM-derived TWS is 0.71, 0.74 and 0.75, respectively. The correlation result is comparable with the correlation of 0.83 reported by Radman et al. (2022) for the TWS and water level of the LU from 2002 to 2019.

The long-term mean monthly variations (Figure 5b) indicate an ascending trend for the water level from January to May when it reaches its maximum level (1272.05 m). The water level diminishes from May to October with the minimum value of 1271.42 m recorded in October. From October to December, a slightly increasing trend is seen in the variations in water level. The temporal correlation between the LU water level and TWS on the mean monthly scale is 0.94, 0.91,0.88 and 0.89 for the JPL, CSR, GSFC and CLSM, respectively.

The lake water volume was estimated considering the area–volume–elevation (AVE) relationship. The variations of the lake's TWS and water volume are given in Figure SM6. The results indicate that from 2003 to 2015 there has been a descending trend in the variations of

TABLE 2 Multiyear (2003–2021) basin-average annual trends of terrestrial water storage (TWS) and groundwater storage (GWS).

		GRACE-JPL	GRACE-CSR	GRACE-GSFC	CLSM
TWS	Trend (mm/year)	−11.50 ± 0.52	−8.82 ± 0.52	−10.22 ± 0.52	−9.75
	Trend (km^3/year)	−0.59 ± 0.03	−0.46 ± 0.03	−0.53 ± 0.03	−0.51
	Total loss (km^3)	−11.20 ± 0.51	−8.74 ± 0.51	−10.07 ± 0.51	−9.69
GWS	Trend (mm/year)	−9.10 ± 0.68	−6.32 ± 0.68	−7.72 ± 0.68	−10.20
	Trend (km^3/year)	−0.47 ± 0.03	−0.33 ± 0.03	−0.40 ± 0.03	−0.53
	Total loss (km^3)	−8.87 ± 0.67	−6.22 ± 0.67	−7.60 ± 0.67	−10.10

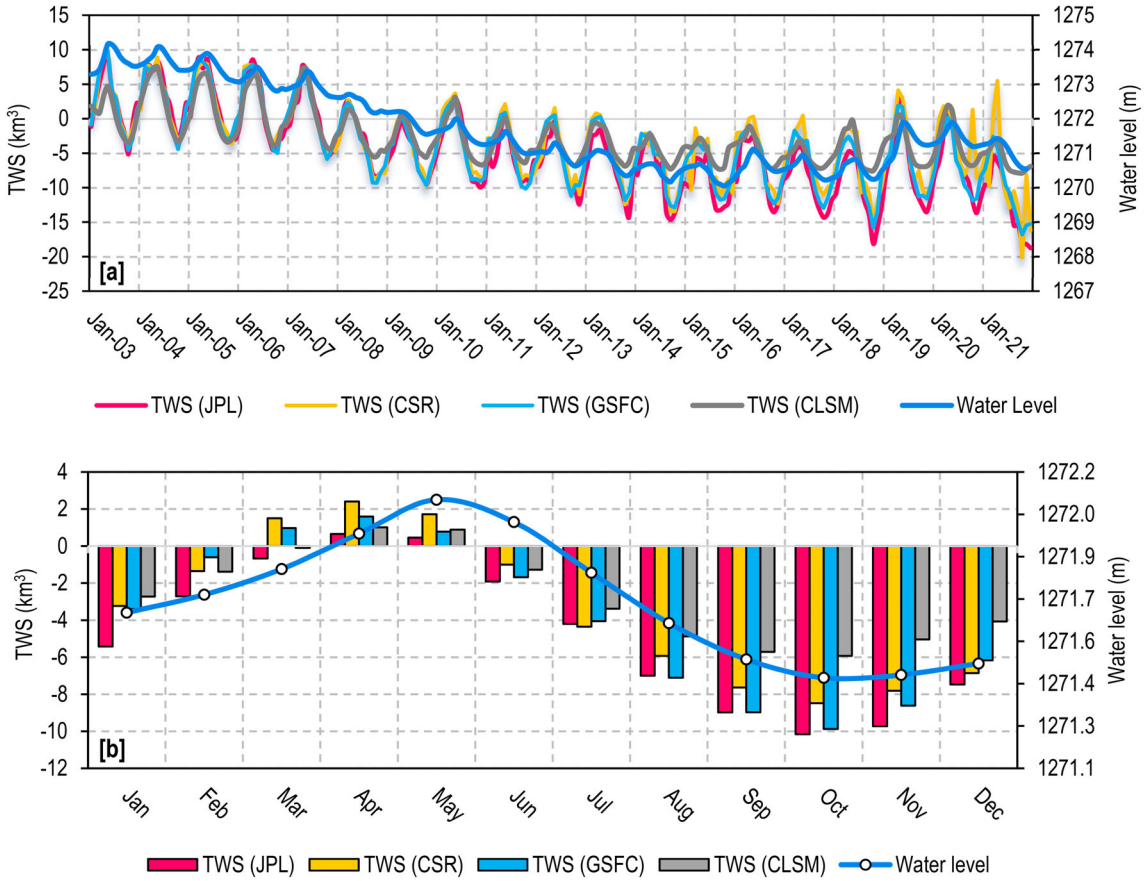

FIGURE 5 Multiyear (2003–2021) monthly (a), mean-monthly, and (b) associations between terrestrial water storage (TWS), and sea level variations.

the lake volume, during which the volume of the lake decreased from 14.03 km^3 in 2003 to 2.0 km^3 in 2015 meaning that the LU has lost about 86% of its volume in this period. This is in accordance with the findings of Darehshouri et al. (2023). There is a slight increase in the lake volume from 2019 to 2020 mainly due to the restoration measures. The results also suggest that, on average, there is a high association between lake volume and TWS with a correlation of 0.76.

3.9 | Parameters affecting the desiccation process

3.9.1 | Hydrometeorological extremes

For investigating the hydrometeorological situation of the LUB, two drought metrics (scPDSI and 12-month SPEI) were used. The basin-average variations of the scPDSI and SPEI-12 (Figure 6) demonstrate that several drought incidents have been felt in the LUB from 2003 to 2021. The first and most severe event was between 2008 and 2009. The major drought in the year 2008 was also distinguished by Saemian et al. (2020). The scPDSI-based results suggest moderate droughts in 2010–2011, 2014 and 2017 while SPEI-12 shows drought events in 2010–2011, 2017 and 2021. The moderately dry periods in 2010 and 2017 were also reported by Mirgol et al. (2021).

The impact of the experienced droughts on the variations of TWS, GWS and the lake's water level was also investigated. It is apparent that especially in 2008, the drought affected the water storage of the basin when a sharp decrease in the variations of TWS and GWS was observed. The indices also indicate a wet period in 2019–2020 with positive values, which are in agreement with the increasing trend of the TWS and GWS at the same time. However, a trivial

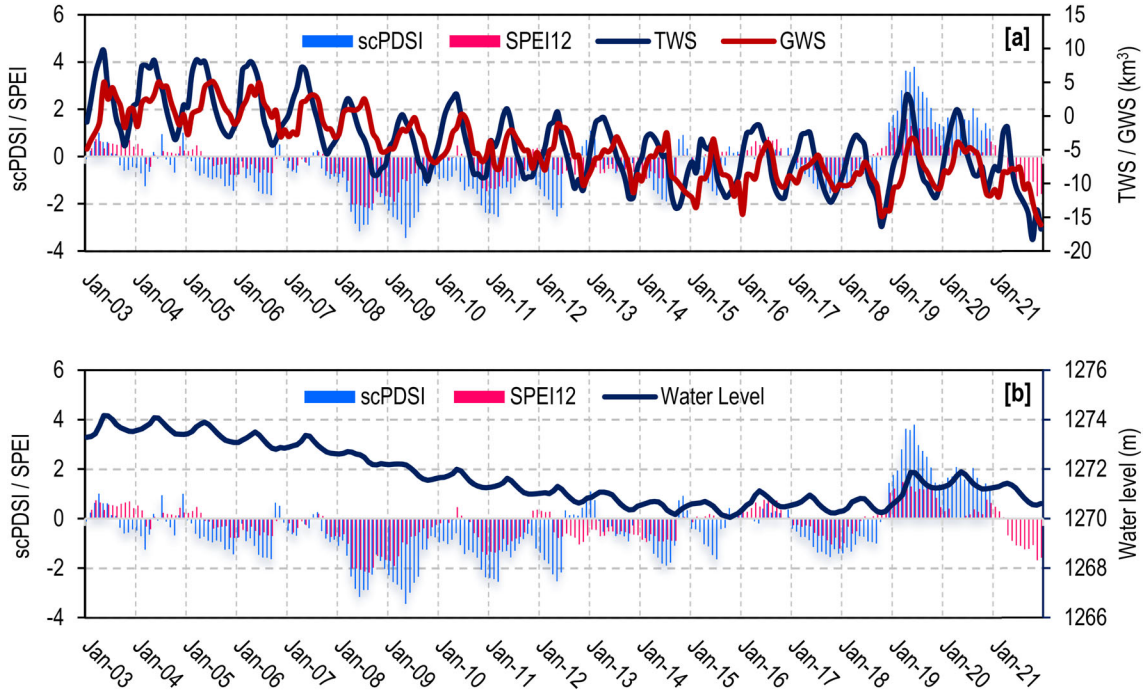

FIGURE 6 Multiyear (2003–2021) monthly associations of drought metrics with terrestrial water storage (TWS), groundwater storage (GWS) (a) and the lake's water level (b).

association between the scPDSI and SPEI with the variations in water level is seen (Figure 6b). But from the overall viewpoint and based on the variations of drought indices, the decreasing trend of the water table from 2008 can be associated with the unfavourable climatic conditions of the area since the climatic situation of the basin seems critical from 2008 onward.

The hydrological status of the basin was further characterized based on the temporal time series of the anomalies of the TWS, precipitation (P) and storage deficit (SD) of the soil (Figure 7). The storage deficit (SD) is the amount of storable water in the soil layer that can be held before achieving maximum storage and was calculated according to Khorrami, Fistikoglu, and Gunduz (2022). The hydrological status (Figure 7) of the LUB illustrates the relationship between the TWS with the SD and P over the LUB where the increases in precipitation are responsible for the increase in the TWS, while the storage deficit is decreasing. It is interpreted such that there is a high inundation potentiality at the intersection points of these variables on the graph (Idowu, 2021). During the dry periods, the vertical gap between these variables extremely increases especially for the prolonged gap between the SD and TWS. In this premise, it can be inferred that in May 2003, March 2005, March 2006 and April 2007, the LUB has been susceptible to flood events. From 2008 onward, on the other hand, the basin has experienced harsh hydrological conditions.

3.9.2 | Anthropogenic forces

Human intervention is another effective parameter of the desiccation of the LU. It is stated that about 89% of the total water consumption in the LUB appertains to the agricultural sector while the remaining 11% of the water is used by the industry and domestic sectors (Wurtsbaugh & Sima, 2022). To investigate the impacts of the anthropogenic forces on the variations of water storage and the lake's water level, the total water use (TWU) in the LUB was extracted from the WaterGAP hydrology model from 2003 to 2015. TWU accounts for water consumption from both surface and subsurface resources. The variations of TWU and its association with TWS and GWS (Figure 8) suggest that there is a high correlation between them over the LUB. The correlation between the TWU and TWS and GWS is −0.61 and −0.51, respectively. It is found that TWU agrees with TWS and GWS within a temporal lag of three and 4 months, respectively.

From the water balance perspective, it is expressed that the variations of TWS over endorheic basins are mainly affected by the variations of P and ET (Yang et al., 2021). TWS in such basins is subjected to huge losses on account of anthropogenic drivers such as agricultural irrigation, dam construction, and groundwater extraction, through which water storage is lost by ET to the atmosphere (Pan et al., 2017). To quantify the human-induced water storage loss, the TWS changes (TWSC) and ET from GRACE were compared to the model-based ET and TWS. TWSC is calculated as the temporal derivative of TWSA from the GRACE products. The TWSC for each month is estimated as the differential of two consecutive months of TWSA at the beginning of a month (see Khorrami et al., 2023). The net water flux is expressed in terms of the differences between P and ET (P-ET) (Yang et al., 2021), which represents the TWS of the basin. The temporal variations of TWS changes (Figure 9a) suggest that there is a high agreement between the GRACE-TWS and P-ET over the LUB with a correlation of 0.78. Tourian et al. (2015) and Saemian et al.

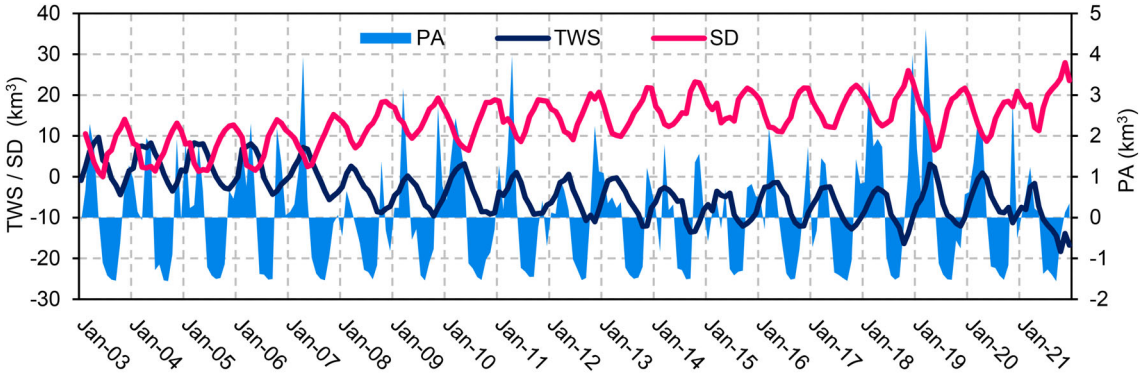

FIGURE 7 Hydrological status of the Lake Urmia basin (LUB).

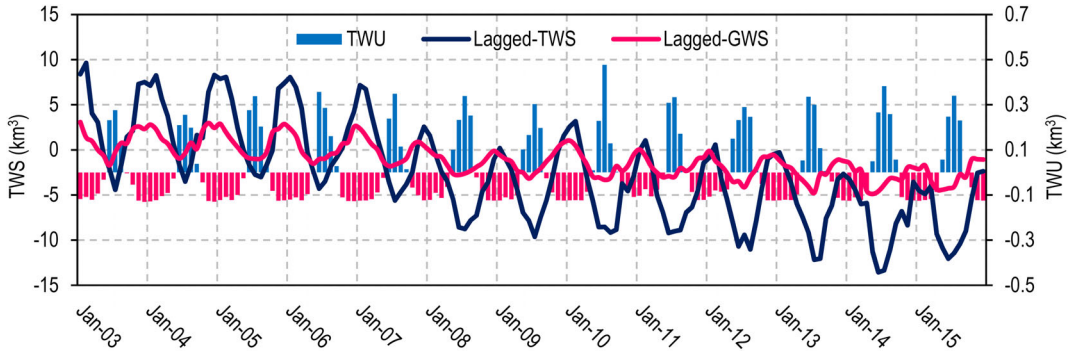

FIGURE 8 Temporal illustration of the water abstraction impacts on the variations of terrestrial water storage (TWS) and groundwater storage (GWS) over the Lake Urmia basin (LUB).

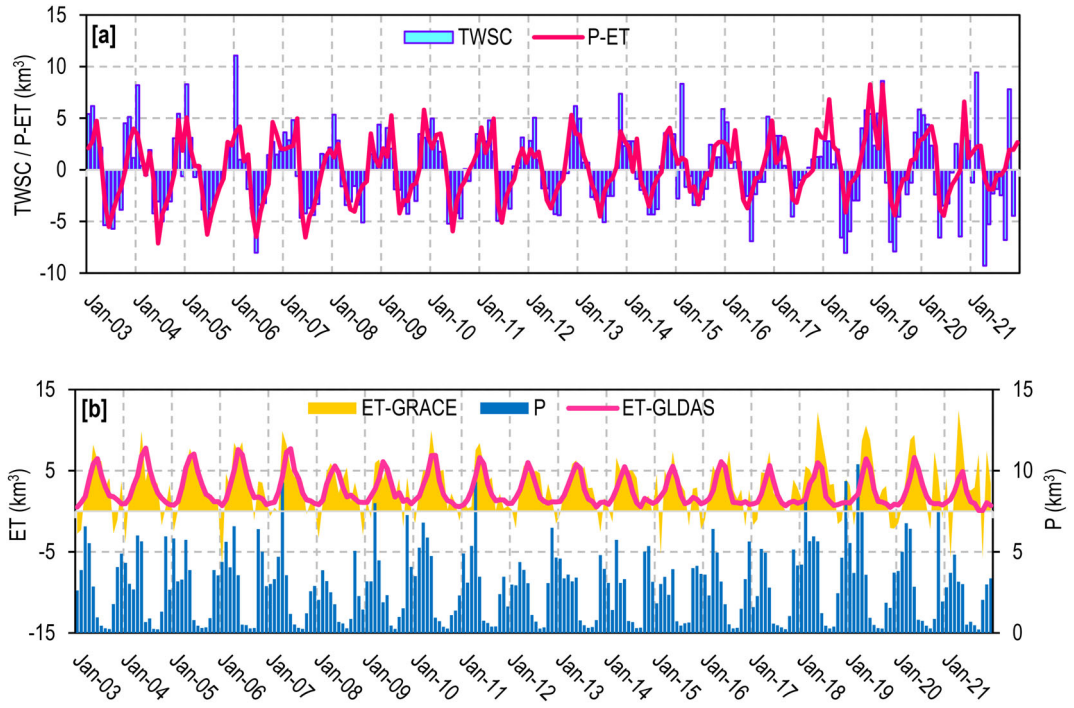

FIGURE 9 Variations in terrestrial water storage change (TWSC), $(P-\mathrm{ET})_{\mathrm{GLDAS}}$ (a), and ET-GRACE, ET-GLDAS, and P (b) from 2003 to 2021.

(2020) reported a correlation of 0.73, and 0.86 for the GRACE and P-ET associations over the LUB, respectively. Figure 9b, on the other hand, illustrates the variations of P and ET over the LUB. The variations of the GRACE-ET are in good harmony with those of the GLDAS-ET ($R = 0.70$). It is also found that ET affects the variations of TWS adversely with a correlation of −0.82 suggesting the harsh impacts of the anthropogenic forces on the water storage changes in the LUB. According to Feizizadeh et al. (2022), a substantial increase is seen in the area of croplands and agricultural areas from 2005 to 2015, which contributed to the desiccation of the LU through increasing the water demand and extraction from the nearby aquifers for farmland irrigation.

3.10 | Spatial assessment

The thematic maps of the mean annual values of the hydrological parameters (Figure 10) were drawn to better illustrate the situation of the LUB from the viewpoint of the spatial variability of the parameters. The spatial variations of TWS and GWS show the same pattern with the least decreasing water storage over the northern parts while it diminishes more towards the east and south of the basin. It indicates that the LUB has lost at most an estimated mean volume of 6.50 and 5.90 km^3 of its TWS and GWS, respectively, through the last 19 years from 2003 to 2021. The maximum loss of water storage of the basin over its southern parts corresponds exactly with the

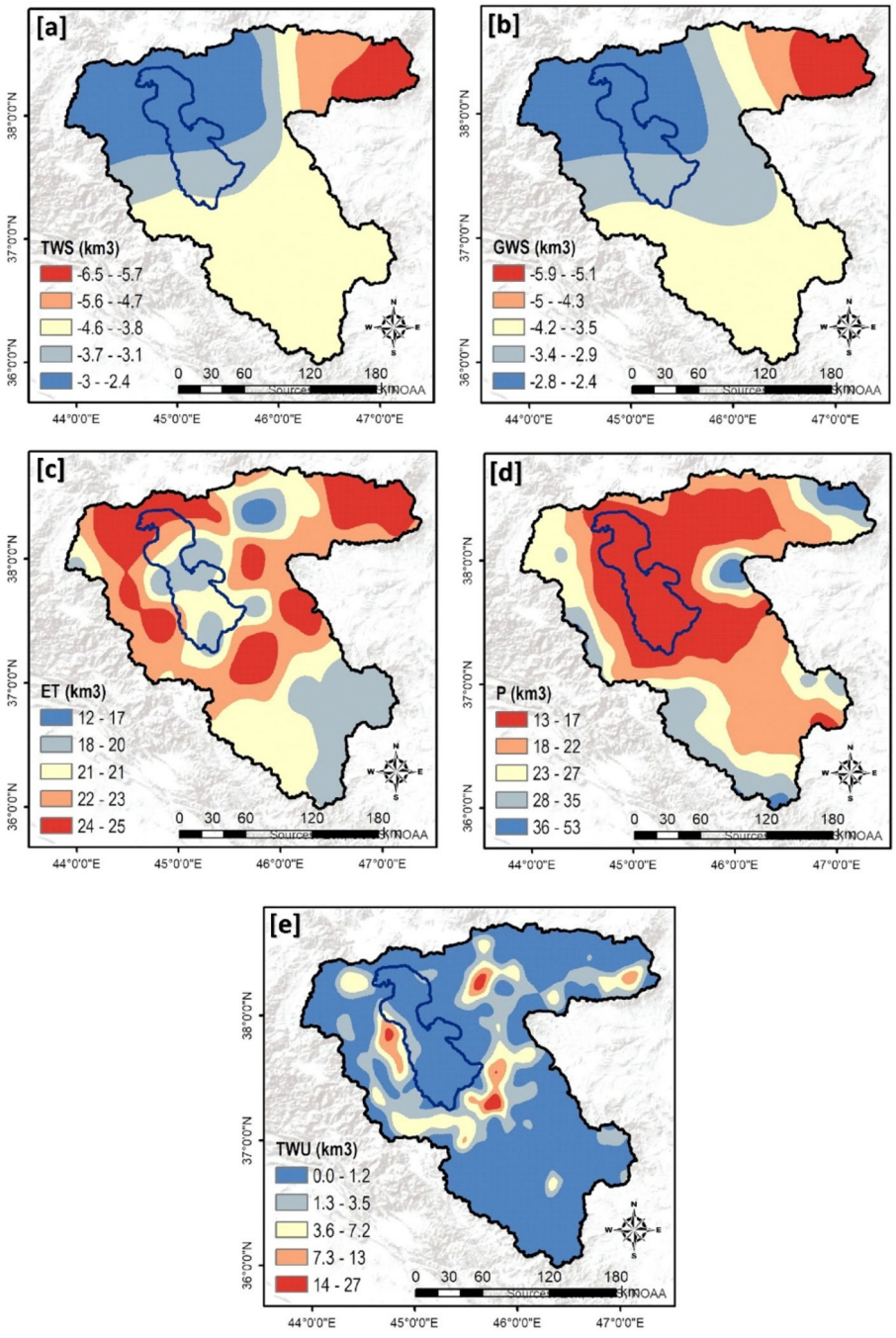

FIGURE 10 Spatial distribution of the mean annual terrestrial water storage (a), groundwater storage (b), evapotranspiration (c), precipitation (d), and total water use (e).

desiccation pattern of the LU (Figure 1) where the southern parts of the LU have been affected the most by the desiccation process than the northern parts. The mean annual variations of P also suggest that the central LUB, especially the LU area, receives the least water from precipitation, which varies between 13 to 17 km^3 annually. While the elevated areas receive the maximum precipitation reaching 53 km^3 of the annual P. Variations of the annual ET demonstrate more water loss from the areas around the lake. The ET variability indicates that the LUB loses at most 25 km^3 of its water storage from ET each year. Overall, it is found that the ET exceeds P in the LUB. While the annual amount of precipitation is 20.54 km^3, it loses about 21.50 km^3 through evapotranspiration suggesting the existence of a negative hydrological balance of -0.96 km^3 over the LUB, which is an alarming dry condition during the study period. The negative balance between P and ET was also reported by Barideh and Nasimi (2022) who estimated a negative balance of -0.67 km^3 for the time period of 2009 to 2020 with the mean annual ET and P of 15.92 and 15.24 km^3, respectively. The spatial variability of TWU over the LUB also implies that water consumption mostly occurs around the LU, which corresponds to the agricultural and residential areas. It reveals that on average, the LUB has lost about 1.38 km^3 of its annual storage through water consumption from 2003 to 2015.

4 | DISCUSSION

4.1 | Pros and cons of the STL gap filling

There are several techniques suggested for reconstructing the missing values of the GRACE mission. The STL-based gap-filling approach proposed in this study takes the benefit of the seasonal variations of the GRACE-observed TWS. Seasonality is a general aspect of the global TWS variations, and the STL works based on the decomposition of the temporal variations of TWS to come up with the missing data. STL is in fact a filtering technique for the decomposition of time-series datasets. It is simple and at the same time robust. In this study, the STL-derived TWS values correlated well with the existing model-based TWS values over the LUB, whose feasibility can be further verified by comparing to the findings of Soltani and Azari (2022) that reported a correlation of 0.73 for the simulated TWS using GMDH machine learning technique. The simplicity of the STL paves the way for the fast computation and analysis of very large time series data (Cleveland et al., 1990). The main merit of the new proposed STL-based gap-filling technique over the previously tested methods lies in its ability to give accurate predictions of the GRACE gaps more straightforwardly and conveniently compared to other techniques. However, the main handicap of the STL technique is that it can be applied to a temporal domain rather than spatial data.

4.2 | Performance of the drought metrics

To investigate the experienced drought incidents and their association with the water storage and the lake's water level variations over the LUB, two traditional drought indicators of scPDSI and SPEI are used in this study. Although the Standardized Precipitation Index (SPI) is overwhelmingly utilized through the majority of drought evaluation studies, the authors ignored using it over the LUB because it was suggested that SPEI outperforms SPI in the LUB (Mirgol et al., 2021). It can be justified based on the fact that the LUB is more affected by increasing temperature and ET impacts rather than precipitation variations themselves (Mirgol et al., 2021). Thus, SPEI and scPDSI, for which ET are included in the calculation process (Khorrami & Gündüz, 2022; van der Schrier et al., 2013), can yield better results compared to SPI. Since the traditional drought indices rely mainly on the accumulation of precipitation deficits, they are lame to capture the hydrological condition of a region and the extent of drought influence on subsurface hydrology (Thomas et al., 2014). From this perspective, the low association between the time series of scPDSI and SPEI and TWS and GWS over the LUB can be justified. Furthermore, the meteorological droughts, identified by scPDSI, and SPEI, are different from the water storage (TWS and GWS) in timing due to the inherent lags within the hydrologic system (Thomas et al., 2014).

4.3 | Uncertainties involved

In the current study, several uncertainty sources were engaged in the analysis. To get rid of the uncertainty induced by the GRACE data processing errors, the modern Mascon solution data was applied instead, which is proven to be superior to the alternative spherical harmonics data (Aryal & Zhu, 2020). However, there are also uncertainties associated with the Mascon solutions on account of the used diverse background models as well as data processing approaches (Kumar et al., 2021). The other source of the uncertainties of the results is the simulation errors of the global models such as Noah and CLSM. One solution to diminish the uncertainties ascribed to hydrological model outputs is to use the ensemble mean of several models (Cao et al., 2015). Thus, the Noah and CLSM-derived parameters emerged to reduce the uncertainty of the results.

5 | CONCLUSIONS AND RECOMMENDATIONS

Lake Urmia is among the most critical water bodies of Iran playing a predominant role in the stability of the microclimate of the northwestern regions of the country. Unfortunately, long-term impacts of both natural and man-made forces have contributed to the loss of its hydrological balance resulting in the damage of the lake and its surrounding societies as well. The desiccation of the lake has triggered the exposure of more salt in time, which is likely to be dispersed throughout the region via potential storms. Since the economy of the inhabitants of the NW of Iran is mainly based on agriculture, it is believed that the continuation of the current drying process will jeopardize the lives of millions of people in the country with its catastrophic socio-economic side effects.

Within the scope of the current study, several remote sensing data including the GRACE/GRACE-FO satellite estimates, hydrological and climatic model outputs as well as in-situ observations were jointly used to evaluate the recent hydrological dynamics of the LU. Because the GRACE data have missing data months, the STL-based gap-filling approach was proposed as a new method to reconstruct the GRACE-derived TWS for the missed months. The findings cast light on the high feasibility of the proposed technique in predicting the missing TWS values of the GRACE missions. However, since it is performed for the temporal data, the authors aim at improving the proposed STL method for filling in the spatial gaps as well.

The findings of this study ascribe the dissipation of the LU to both natural and anthropogenic forces suggesting that both climate crisis and human intervention are involved in the desiccation process of the LU while stressing the dominant impact of evaporation of the water storage of the region on the drying of the lake. It was found that the excessive water loss through the evaporation process during the last decades has culminated in an alarming negative hydrological balance over the LUB, which exacerbates the drying process. Therefore, any countermeasures implemented by the local authorities should take this hydrological status into account to achieve more effective outcomes.

ACKNOWLEDGEMENTS

The third co-author is financially sponsored by the Higher Education Council of Türkiye through 100/2000 PhD Scholarship Program.

CONFLICT OF INTEREST STATEMENT

The authors declare that they have no known competing financial interests or personal relationships that could have appeared to influence the work reported in this paper.

DATA AVAILABILITY STATEMENT

The data that support the findings of this study are available from the corresponding author upon reasonable request.

ORCID

Behnam Khorrami https://orcid.org/0000-0003-3265-372X
Shoaib Ali https://orcid.org/0000-0003-1390-0377
Onur Gungor Sahin https://orcid.org/0000-0002-0502-1033
Orhan Gunduz https://orcid.org/0000-0001-6302-0277

REFERENCES

Alcamo, J., Döll, P., Henrichs, T., Kaspar, F., Lehner, B., Rösch, T., & Siebert, S. (2003). Development and testing of the WaterGAP 2 global model of water use and availability. *Hydrological Sciences Journal*, *48*, 317–338. https://doi.org/10.1623/hysj.48.3.317.45290

Alhaji, U. U., Yusuf, A. S., Edet, C. O., Oche, C. O., & Agbo, E. P. (2018). Trend analysis of temperature in Gombe state using Mann Kendall trend test. *Journal of Scientific Research & Reports*, *20*(3), 1–9.

Aryal, Y., & Zhu, J. (2020). Multimodel ensemble projection of meteorological drought scenarios and connection with climate based on spectral analysis. *International Journal of Climatology*, *40*(7), 3360–3379. https://doi.org/10.1002/joc.6402

Azizpour, J., & Ghaffari, P. (2021). Global and regional signals in the water level variation in Hypersaline Basin of the Lake Urmia. In *The handbook of environmental chemistry*. Springer. https://doi.org/10.1007/698_2021_739

Banihabib, M. E., Azarnivand, A., & Peralta, R. C. (2015). A new framework for strategic planning to stabilize a shrinking lake. *Lake and Reservoir Management*, *31*(1), 31–43. https://doi.org/10.1080/10402381.2014.987409

Barideh, R., & Nasimi, F. (2022). Investigating the changes in agricultural land use and actual evapotranspiration of the Urmia Lake basin based on FAO's WaPOR database. *Agricultural Water Management*, *264*, 107509. https://doi.org/10.1016/j.agwat.2022.107509

Beguería, S., Vicente-Serrano, S. M., & Angulo-Martínez, M. (2010). A multiscalar global drought dataset: The SPEIbase: A new gridded product for the analysis of drought variability and impacts. *Bulletin of the American Meteorological Society*, *91*(10), 1351–1354. https://doi.org/10.1175/2010BAMS2988.1

Briffa, K. R., van der Schrier, G., & Jones, P. D. (2009). Wet and dry summers in Europe since 1750: Evidence of increasing drought. *International Journal of Climatology: A Journal of the Royal Meteorological Society*, *29*(13), 1894–1905. https://doi.org/10.1002/joc.1836

Cao, Y., Nan, Z., & Cheng, G. (2015). GRACE gravity satellite observations of terrestrial water storage changes for drought characterization in the arid land of northwestern China. *Remote Sensing*, *7*(1), 1021–1047. https://doi.org/10.3390/rs70101021

Cleveland, R. B., Cleveland, W. S., McRae, J. E., & Terpenning, I. (1990). STL: A seasonal-trend decomposition. *Journal of Official Statistics*, *6*(1), 3–73.

Darehshouri, S., Michelsen, N., Schüth, C., Tajrishy, M., & Schulz, S. (2023). Evaporation from the dried-up Lake bed of Lake Urmia, Iran. *Science of the Total Environment*, *858*, 159960.

Farajzadeh, J., Fard, A. F., & Lotfi, S. (2014). Modeling of monthly rainfall and runoff of Urmia lake basin using "feed-forward neural network" and "time series analysis" model. *Water Resources and Industry*, *7*, 38–48. https://doi.org/10.1016/j.wri.2014.10.003

Fathian, F., Morid, S., & Kahya, E. (2015). Identification of trends in hydrological and climatic variables in Urmia Lake basin, Iran. *Theoretical and Applied Climatology*, *119*(3), 443–464. https://doi.org/10.1007/s00704-014-1120-4

Feizizadeh, B., Lakes, T., Omarzadeh, D., Sharifi, A., Blaschke, T., & Karimzadeh, S. (2022). Scenario-based analysis of the impacts of Lake drying on food production in the lake Urmia Basin of northern Iran. *Scientific Reports*, *12*(1), 6237.

Feizizadeh, B., Mohammadzade Alajujeh, K., Lakes, T., Blaschke, T., & Omarzadeh, D. (2021). A comparison of the integrated fuzzy object-based deep learning approach and three machine learning techniques for land use/cover change monitoring and environmental impacts assessment. *GIScience & Remote Sensing*, *58*(8), 1543–1570. https://doi.org/10.1080/15481603.2021.2000350

Flechtner, F., Morton, P., Watkins, M., & Webb, F. (2014). Status of the GRACE follow-on Mission. In U. Marti (Ed.), *Proceedings of the gravity, geoid and height systems* (pp. 117–121). Springer International Publishing.

Forootan, E., Rietbroek, R., Kusche, J., Sharifi, M. A., Awange, J. L., Schmidt, M., Omondi, P., & Famiglietti, J. (2014). Separation of large-scale water storage patterns over Iran using GRACE, altimetry and hydrological data. *Remote Sensing of Environment*, *140*, 580–595. https://doi.org/10.1016/j.rse.2013.09.025

Girotto, M., Reichle, R., Rodell, M., & Maggioni, V. (2021). Data assimilation of terrestrial water storage observations to estimate precipitation fluxes: A synthetic experiment. *Remote Sensing*, *13*(6), 1223. https://doi.org/10.3390/rs13061223

Hosseini-Moghari, S. M., Araghinejad, S., Tourian, M. J., Ebrahimi, K., & Döll, P. (2020). Quantifying the impacts of human water use and climate variations on recent drying of Lake Urmia basin: The value of

different sets of spaceborne and in situ data for calibrating a global hydrological model. *Hydrology and Earth System Sciences*, *24*(4), 1939–1956. https://doi.org/10.5194/hess-24-1939-2020

Hu, Z., Zhou, Q., Chen, X., Chen, D., Li, J., Guo, M., & Duan, Z. (2019). Groundwater depletion estimated from GRACE: A challenge of sustainable development in an arid region of Central Asia. *Remote Sensing*, *11*(16), 1908. https://doi.org/10.3390/rs11161908

Humphrey, V., Gudmundsson, L., & Seneviratne, S. I. (2016). Assessing global water storage variability from GRACE: Trends, seasonal cycle, subseasonal anomalies and extremes. *Surveys in Geophysics*, *37*(2), 357–395. https://doi.org/10.1007/s10712-016-9367-1

Idowu, D. (2021). Assessing the utilization of remote sensing and GIS techniques for flood studies and land use/land cover analysis through case studies in Nigeria and the USA [Unpublished doctoral dissertation], Colorado School of Mines.

Jalili, S., Kirchner, I., Livingstone, D. M., & Morid, S. (2012). The influence of large-scale atmospheric circulation weather types on variations in the water level of Lake Urmia, Iran. *International Journal of Climatology*, *32*(13), 1990–1996. https://doi.org/10.1002/joc.2422

Kamran, K. V., & Khorrami, B. (2018). Change detection and prediction of Urmia Lake and its surrounding environment during the past 60 years applying geobased remote sensing analysis. International archives of the photogrammetry, remote sensing and spatial. *Information Sciences*, *42*(3/W4), 519–525. https://doi.org/10.5194/isprs-archives-XLII-3-W4-519-2018

Kendall, M. G. (1975). *Rank correlation methods*. Griffin.

Khorrami, B., Ali, S., Abadi, L. H., & Jehanzaib, M. (2022). Spatio-temporal variations in characteristics of terrestrial water storage and associated drought over different geographic regions of Türkiye. *Earth Science Informatics*, *2022*, 717–731. https://doi.org/10.1007/s12145-022-00907-3

Khorrami, B., Arik, F., & Gunduz, O. (2021). Land deformation and sinkhole occurrence in response to the fluctuations of groundwater storage: An integrated assessment of GRACE gravity measurements, ICESat/ICESat-2 altimetry data and hydrologic models. *GIScience & Remote Sensing*, *58*(8), 1518–1542. https://doi.org/10.1080/15481603.2021.2000349

Khorrami, B., Fistikoglu, O., & Gunduz, O. (2022). A systematic assessment of flooding potential in a semi-arid basin using GRACE gravity estimates and large-scale hydrological modeling. *Geocarto International*, *1-22*, 11030–11051. https://doi.org/10.1080/10106049.2022.2045365

Khorrami, B., Gorjifard, S., Ali, S., & Feizizadeh, B. (2023). Local-scale monitoring of evapotranspiration based on downscaled GRACE observations and remotely sensed data: An application of terrestrial water balance approach. *Earth Science Informatics*. https://doi.org/10.1007/s12145-023-00964-2

Khorrami, B., & Gunduz, O. (2019). Analyses of meteorological drought and its impacts on groundwater fluctuations, a case study: Marand plain (Iran). *Pamukkale University Journal of Engineering Sciences*, *25*(6), 711–717. https://doi.org/10.5505/pajes.2019.63600

Khorrami, B., & Gunduz, O. (2021a). Evaluation of the temporal variations of groundwater storage and its interactions with climatic variables using GRACE data and hydrological models: A study from Turkey. *Hydrological Processes*, *35*(3), e14076. https://doi.org/10.1002/hyp.14076

Khorrami, B., & Gunduz, O. (2021b). An enhanced water storage deficit index (EWSDI) for drought detection using GRACE gravity estimates. *Journal of Hydrology*, *603*, 126812. https://doi.org/10.1016/j.jhydrol.2021.126812

Khorrami, B., & Gündüz, O. (2022). Detection and analysis of drought over Turkey with remote sensing and model-based drought indices. *Geocarto International*, *1-23*, 12171–12193. https://doi.org/10.1080/10106049.2022.2066197

Kumar, K. S., AnandRaj, P., Sreelatha, K., Bisht, D. S., & Sridhar, V. (2021). Monthly and seasonal drought characterization using grace-based groundwater drought index and its link to teleconnections across South Indian River basins. *Climate*, *9*(4), 56. https://doi.org/10.3390/cli9040056

Kumar, S. V., Zaitchik, B. F., Peters-Lidard, C. D., Rodell, M., Reichle, R., Li, B., Jasinski, M., Mocko, D., Getirana, A., De Lannoy, G., Cosh, M. H., Hain, C. R., Anderson, M., Arsenault, K. R., Xia, Y., & Ek, M. (2016). Assimilation of gridded GRACE terrestrial water storage estimates in the north American land data assimilation system. *Journal of Hydrometeorology*, *17*(7), 1951–1972. https://doi.org/10.1175/JHM-D-15-0157.1

Lai, Y., Zhang, B., Yao, Y., Liu, L., Yan, X., He, Y., & Ou, S. (2022). Reconstructing the data gap between GRACE and GRACE follow-on at the basin scale using artificial neural network. *Science of the Total Environment*, *823*, 153770. https://doi.org/10.1016/j.scitotenv.2022.153770

Li, F., Kusche, J., Rietbroek, R., Wang, Z., Forootan, E., Schulze, K., & Lück, C. (2020). Comparison of data-driven techniques to reconstruct (1992–2002) and predict (2017–2018) GRACE-like gridded total water storage changes using climate inputs. *Water Resources Research*, *56*(5), e2019WR026551. https://doi.org/10.1029/2019WR026551

Madani, K., AghaKouchak, A., & Mirchi, A. (2016). Iran's socio-economic drought: Challenges of a water-bankrupt nation. *Iranian Studies*, *49*(6), 997–1016. https://doi.org/10.1080/00210862.2016.1259286

Mann, H. B. (1945). Nonparametric tests against trend. *Econometrica: Journal of the Econometric Society*, *13*(3), 245–259.

Mirgol, B., Nazari, M., Etedali, H. R., & Zamanian, K. (2021). Past and future drought trends, duration, and frequency in the semi-arid Urmia Lake Basin under a changing climate. *Meteorological Applications*, *28*(4), e2009. https://doi.org/10.1002/met.2009

Mo, S., Zhong, Y., Forootan, E., Mehrnegar, N., Yin, X., Wu, J., Feng, W., & Shi, X. (2022). Bayesian convolutional neural networks for predicting the terrestrial water storage anomalies during GRACE and GRACE-FO gap. *Journal of Hydrology*, *604*, 127244. https://doi.org/10.1016/j.jhydrol.2021.127244

Paca, V. H. D. M., Espinoza-Dávalos, G. E., Moreira, D. M., & Comair, G. (2020). Variability of trends in precipitation across the Amazon River basin determined from the CHIRPS precipitation product and from station records. *Water*, *12*(5), 1244. https://doi.org/10.3390/w12051244

Pan, Y., Zhang, C., Gong, H., Yeh, P. J. F., Shen, Y., Guo, Y., Huang, Z., & Li, X. (2017). Detection of human-induced evapotranspiration using GRACE satellite observations in the Haihe River basin of China. *Geophysical Research Letters*, *44*(1), 190–199. https://doi.org/10.1002/2016GL071287

Portmann, F. (2017). Global irrigation in the 20th century: Extension of the WaterGAP global irrigation model (GIM) with the spatially explicit historical irrigation data set (HID). http://publikationen.ub.uni-frankfurt.de/frontdoor/index/index/docId/44410

Radman, A., Akhoondzadeh, M., & Hosseiny, B. (2022). Monitoring and predicting temporal changes of Urmia Lake and its basin using satellite multi-sensor data and deep-learning algorithms. *Journal of Photogrammetry Remote Sensing and Geoinformation Science*, *90*, 319–335. https://doi.org/10.1007/s41064-022-00203-1

Saemian, P., Elmi, O., Vishwakarma, B. D., Tourian, M. J., & Sneeuw, N. (2020). Analyzing the Lake Urmia restoration progress using ground-based and spaceborne observations. *Science of the Total Environment*, *739*, 139857. https://doi.org/10.1016/j.scitotenv.2020.139857

Sahour, H., Sultan, M., Vazifedan, M., Abdelmohsen, K., Karki, S., Yellich, J. A., Gebremichael, E., Alshehri, F., & Elbayoumi, T. M. (2020). Statistical applications to downscale GRACE-derived terrestrial water storage data and to fill temporal gaps. *Remote Sensing*, *12*(3), 533. https://doi.org/10.3390/rs12030533

Save, H., Bettadpur, S., & Tapley, B. D. (2016). High-resolution CSR GRACE RL05 Mascons. *Journal of Geophysical Research: Solid Earth*, *121*(10), 7547–7569. https://doi.org/10.1002/2016JB013007

Shamsudduha, M., & Taylor, R. G. (2020). Groundwater storage dynamics in the world's large aquifer systems from GRACE: Uncertainty and role

of extreme precipitation. *Earth System Dynamics*, *11*(3), 755–774. https://doi.org/10.5194/esd-11-755-2020

Soltani, K., & Azari, A. (2022). Forecasting groundwater anomaly in the future using satellite information and machine learning. *Journal of Hydrology*, *612*, 128052. https://doi.org/10.1016/j.jhydrol.2022.128052

Sorkhabi, O. M., Asgari, J., & Amiri-Simkooei, A. (2021). Monitoring of Caspian Sea-level changes using deep learning-based 3D reconstruction of GRACE signal. *Measurement*, *174*, 109004. https://doi.org/10.1016/j.measurement.2021.109004

Sun, A. Y., Scanlon, B. R., Save, H., & Rateb, A. (2021). Reconstruction of GRACE total water storage through automated machine learning. *Water Resources Research*, *57*(2), e2020WR028666. https://doi.org/10.1029/2020WR028666

Tabari, H., Marofi, S., Aeini, A., Talaee, P. H., & Mohammadi, K. (2011). Trend analysis of reference evapotranspiration in the western half of Iran. *Agricultural and Forest Meteorology*, *151*(2), 128–136. https://doi.org/10.1016/j.agrformet.2010.09.009

Tangdamrongsub, N., Han, S. C., Tian, S., Müller Schmied, H., Sutanudjaja, E. H., Ran, J., & Feng, W. (2018). Evaluation of groundwater storage variations estimated from GRACE data assimilation and state-of-the-art land surface models in Australia and the North China plain. *Remote Sensing*, *10*(3), 483. https://doi.org/10.3390/rs10030483

Thomas, A. C., Reager, J. T., Famiglietti, J. S., & Rodell, M. (2014). A GRACE-based water storage deficit approach for hydrological drought characterization. *Geophysical Research Letters*, *41*(5), 1537–1545. https://doi.org/10.1002/2014GL059323

Tourian, M. J., Elmi, O., Chen, Q., Devaraju, B., Roohi, S., & Sneeuw, N. (2015). A spaceborne multisensor approach to monitor the desiccation of Lake Urmia in Iran. *Remote Sensing of Environment*, *156*, 349–360. https://doi.org/10.1016/j.rse.2014.10.006

Uz, M., Atman, K. G., Akyilmaz, O., Shum, C. K., Keleş, M., Ay, T., Tandoğdu, B., Zhang, Y., & Mercan, H. (2022). Bridging the gap between GRACE and GRACE-FO missions with deep learning aided water storage simulations. *Science of the Total Environment*, *830*, 154701. https://doi.org/10.1016/j.scitotenv.2022.154701

Vaheddoost, B., & Aksoy, H. (2019). Reconstruction of hydrometeorological data in Lake Urmia basin by frequency domain analysis using additive decomposition. *Water Resources Management*, *33*, 3899–3911.

van der Schrier, G., Barichivich, J., Briffa, K. R., & Jones, P. D. (2013). A scPDSI-based global data set of dry and wet spells for 1901–2009. *Journal of Geophysical Research-Atmospheres*, *118*(10), 4025–4048. https://doi.org/10.1002/jgrd.50355

Wang, F., Shen, Y., Chen, Q., & Wang, W. (2021). Bridging the gap between GRACE and GRACE follow-on monthly gravity field solutions using improved multichannel singular spectrum analysis. *Journal of Hydrology*, *594*, 125972. https://doi.org/10.1016/j.jhydrol.2021.125972

Wurtsbaugh, W. A., & Sima, S. (2022). Contrasting management and fates of two Sister Lakes: Great salt Lake (USA) and Lake Urmia (Iran). *Watermark*, *14*(19), 3005.

Yang, X., Wang, N., Liang, Q., Chen, A. A., & Wu, Y. (2021). Impacts of human activities on the variations in terrestrial water storage of the Aral Sea basin. *Remote Sensing*, *13*(15), 2923. https://doi.org/10.3390/rs13152923

Yi, S., & Sneeuw, N. (2021). Filling the data GapsWithin GRACE missions using singular Spectrum analysis. *Journal of Geophysical Research: Solid Earth*, *126*, e2020JB021227. https://doi.org/10.1029/2020JB021227

Zaitchik, B. F., Rodell, M., & Reichle, R. H. (2008). Assimilation of GRACE terrestrial water storage data into a land surface model: Results for the Mississippi River basin. *Journal of Hydrometeorology*, *9*(3), 535–548. https://doi.org/10.1175/2007JHM951.1

Zeinoddini, M., Tofighi, M. A., & Vafaee, F. (2009). Evaluation of dike-type causeway impacts on the flow and salinity regimes in Urmia Lake, Iran. *Journal of Great Lakes Research*, *35*(1), 13–22. https://doi.org/10.1016/j.jglr.2008.08.001

Zhang, B., Yao, Y., & He, Y. (2022). Bridging the data gap between GRACE and GRACE-FO using artificial neural network in Greenland. *Journal of Hydrology*, *608*, 127614. https://doi.org/10.1016/j.jhydrol.2022.127614

Zhang, X., Li, J., Dong, Q., Wang, Z., Zhang, H., & Liu, X. (2022). Bridging the gap between GRACE and GRACE-FO using a hydrological model. *Science of the Total Environment*, *822*, 153659. https://doi.org/10.1016/j.scitotenv.2022.153659

SUPPORTING INFORMATION

Additional supporting information can be found online in the Supporting Information section at the end of this article.

How to cite this article: Khorrami, B., Ali, S., Sahin, O. G., & Gunduz, O. (2023). Model-coupled GRACE-based analysis of hydrological dynamics of drying Lake Urmia and its basin. *Hydrological Processes*, *37*(5), e14893. https://doi.org/10.1002/hyp.14893